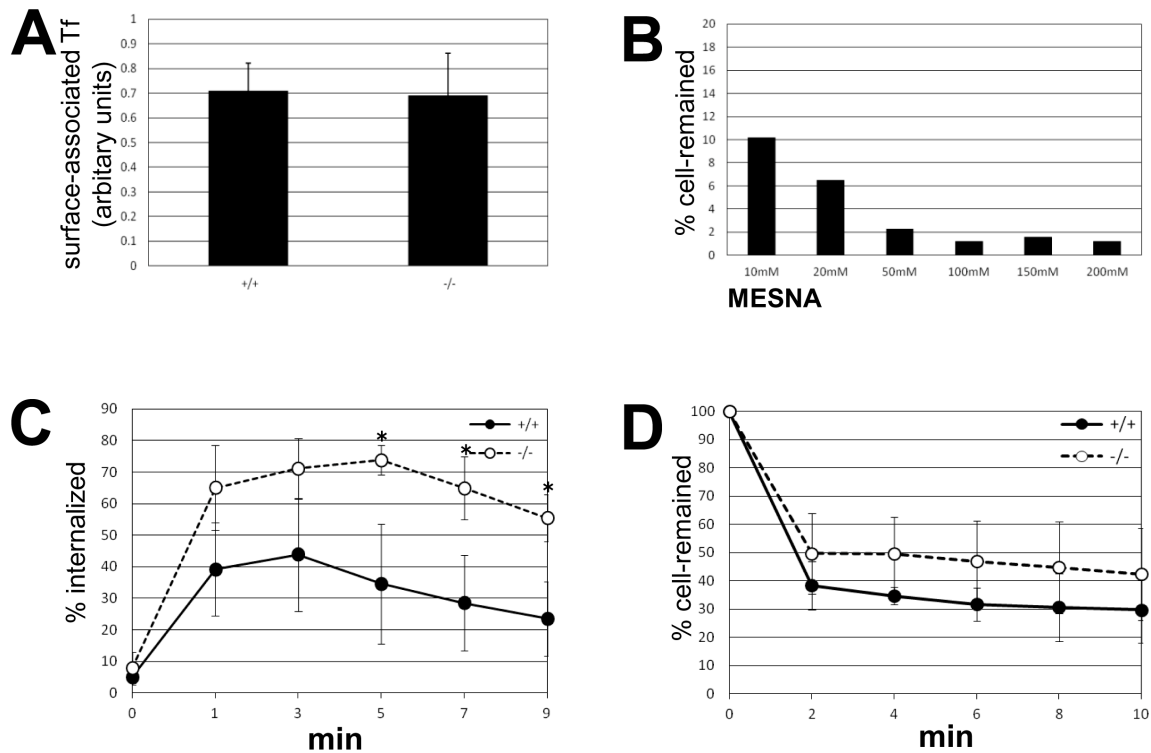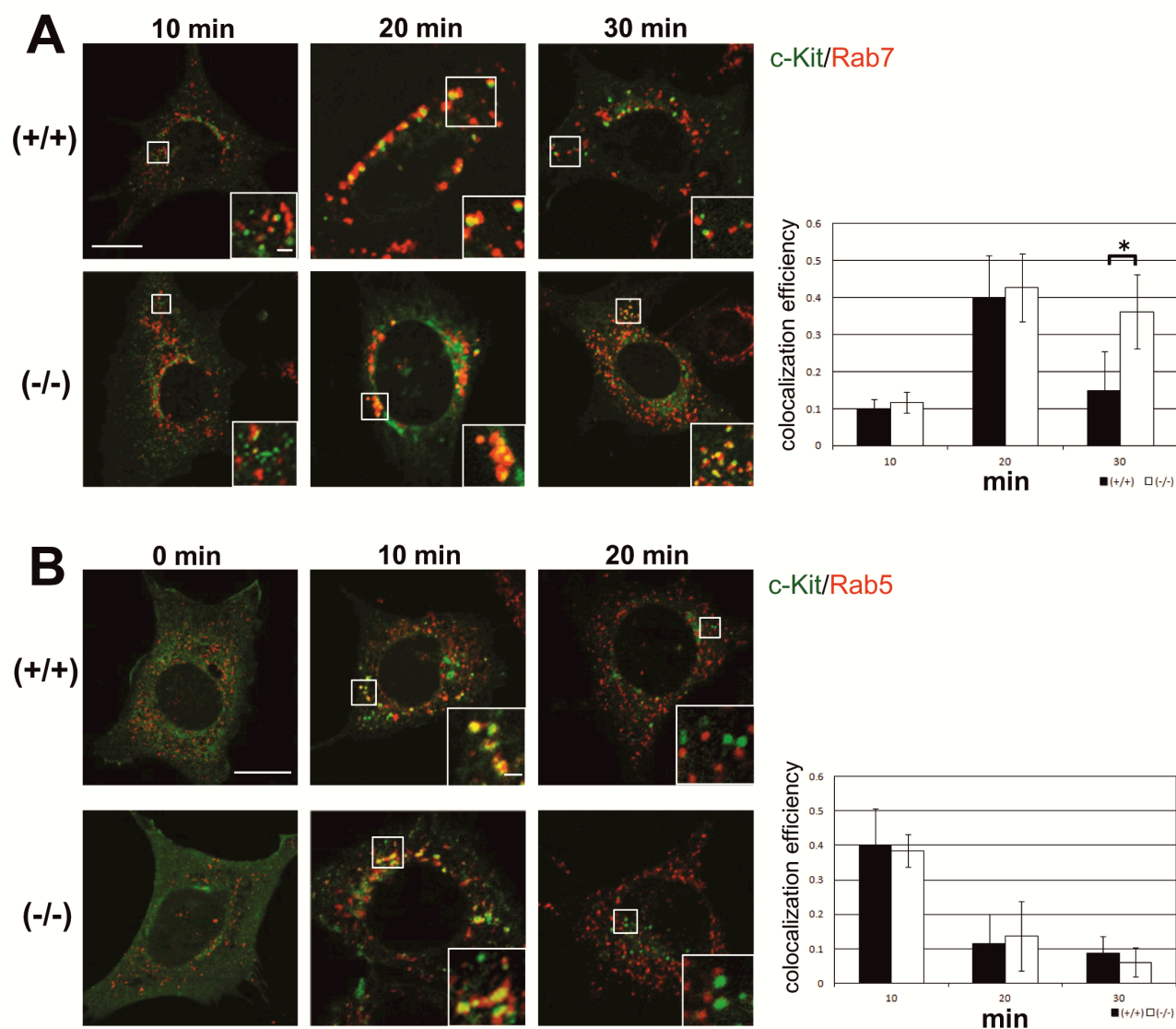**Supplemental data**

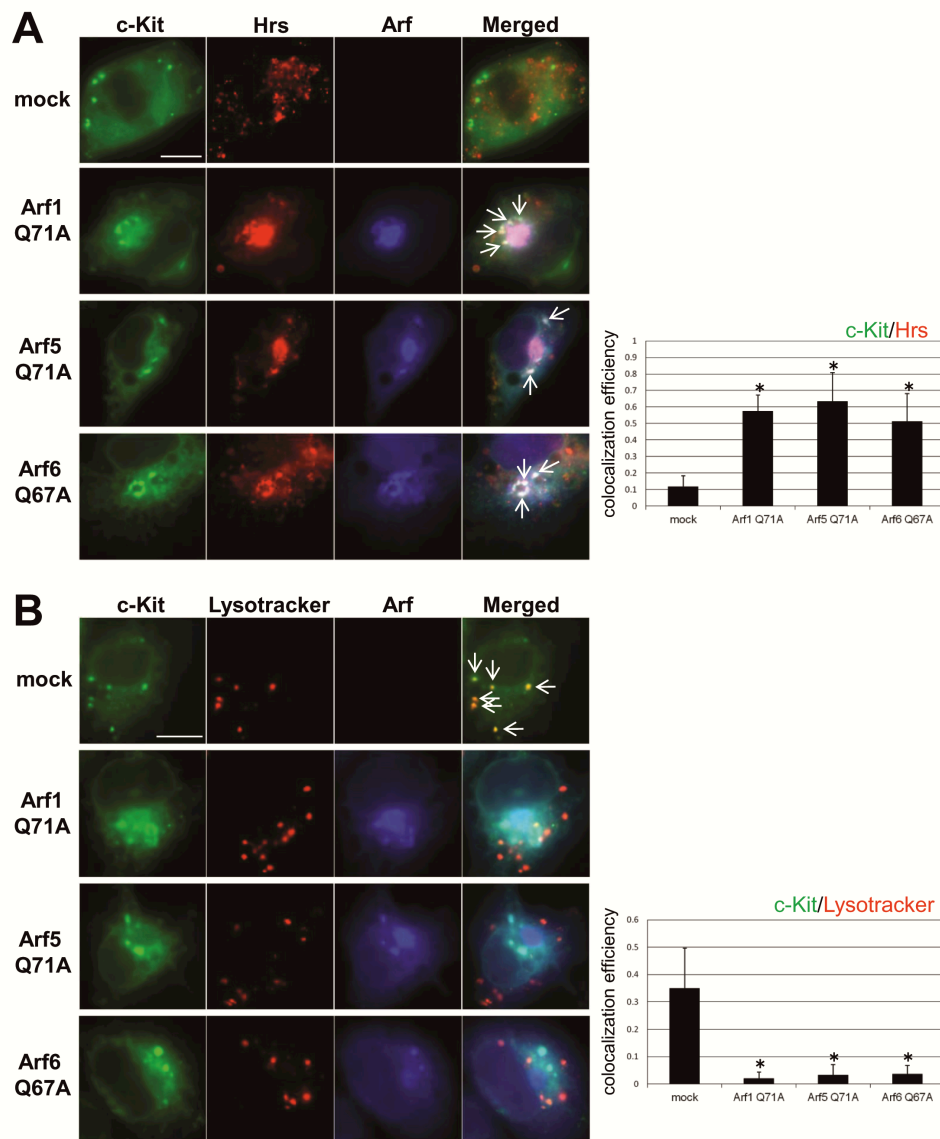*SMAP1* **deficiency perturbs receptor trafficking and predisposes mice to myelodysplasia**

Shunsuke Kon, Naoko Minegishi, Kenji Tanabe, Toshio Watanabe, Tomo Funaki, Won Fen Wong, Daisuke Sakamoto, Yudai Higuchi, Hiroshi Kiyonari, Katsutoshi Asano, Yoichiro Iwakura, Manabu Fukumoto, Motomi Osato, Masashi Sanada, Seishi Ogawa, Takuro Nakamura, and Masanobu Satake
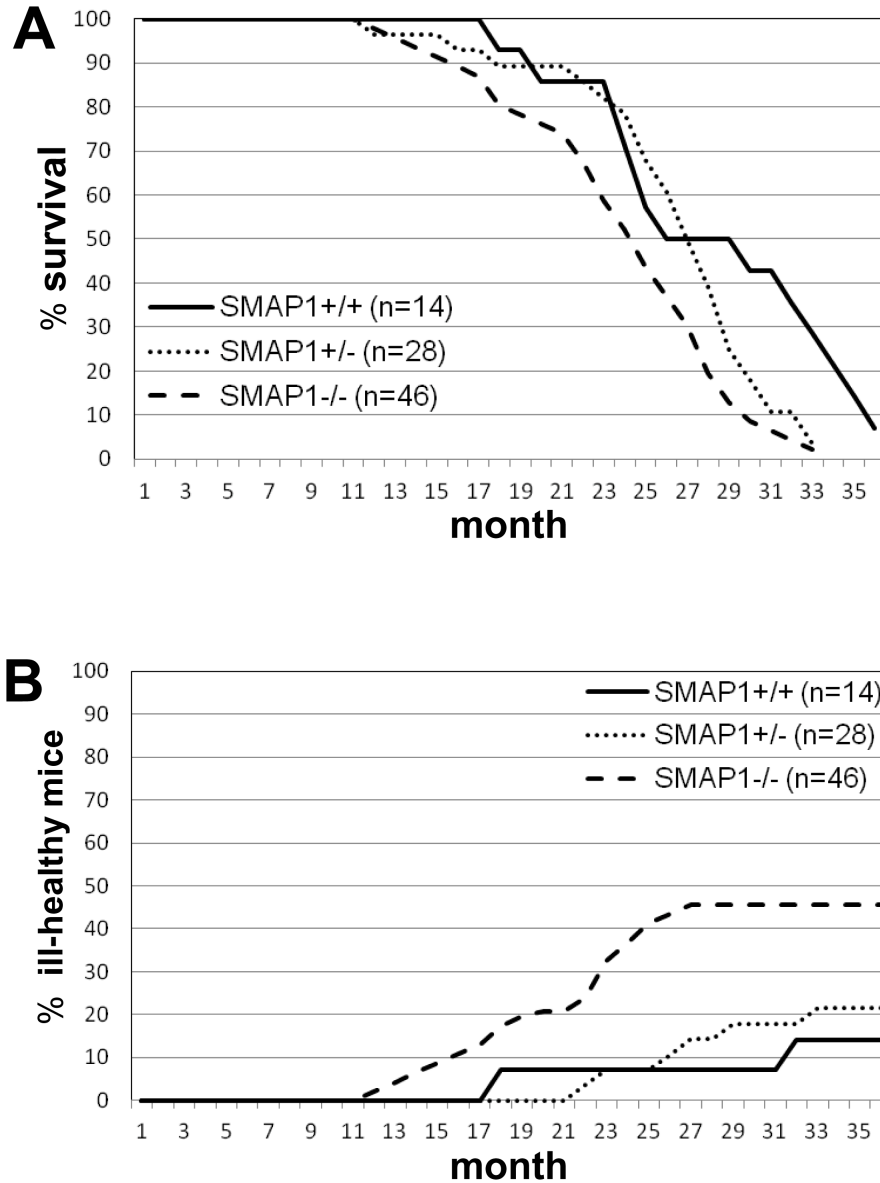
Supplemental Figure 1. Endocytosis and recycling of transferrin as assayed separately in MEFs. **(A)** The *SMAP1*(+/+) and (-/-) MEF lines no. 8 and 7, respectively, were serum-starved, incubated with biotinylated transferrin for 30 min at 4°C, washed and processed for ELISA. The amount of cell surface-bound transferrin is expressed as relative arbitrary units. No significant differences were detected between the two genotypes. **(B)** The surface-bound biotinylated transferrin was stripped by treating cells with the indicated concentrations of sodium 2-mercaptoethane sulfonate (MESNA). The remaining surface transferrin was measured and expressed as a percentage of the initially bound fraction. MESNA at 50 mM effectively removed almost all surface-bound transferrin. **(C)** Transferrin internalization assay. The *SMAP1*(+/+) and (-/-) MEFs were serum-starved, incubated with biotinylated transferrin for 30 min at 4°C, warmed at 37°C for the indicated times, and treated with MESNA. Cell lysates were prepared and processed for ELISA. Internalization of transferrin was enhanced significantly in the *SMAP1*-targeted cells as compared to the wild-type cells. **(D)** Transferrin recycling assay. The *SMAP1*(+/+) and (-/-) MEFs were serum-starved, incubated with biotinylated transferrin at 37°C for 40 min, treated with MESNA, and further incubated at 37°C in the presence of unlabeled transferrin for the indicated period. Cells lysates were prepared and processed for ELISA. No significant differences in the extent of transferrin recycling were detected between the two genotypes. In **(A, C, D)**, independent cultures were prepared in triplicate from the indicated MEF clones, and averages ± sd are shown.
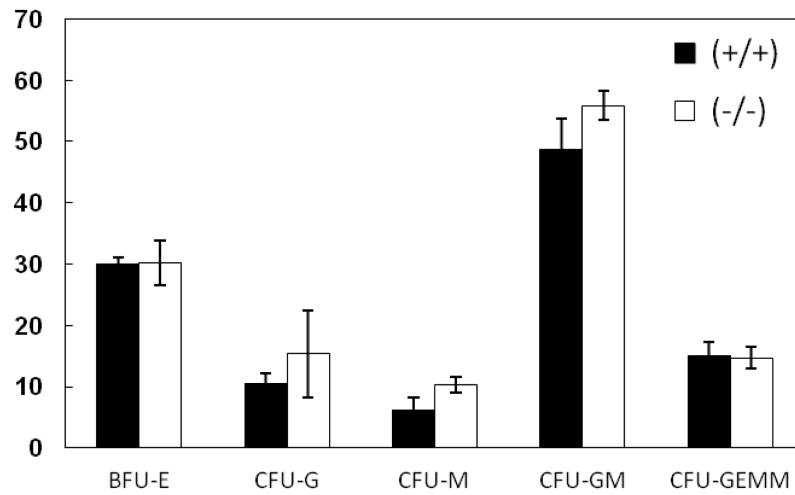
Supplemental Figure 2. Intracellular transport of c-Kit in MEFs. Wild-type and *SMAP1*(-/-) MEFs were transfected by EYFP-c-Kit, incubated with SCF for the indicated times, and processed for double fluorescence detection of c-Kit and Rab7 **(A)** or c-Kit and Rab5 **(B)**. The colocalization of the two molecules was analyzed and plotted as histograms for the indicated incubation periods. Data are shown as averages ± sd (n=50–70). Scale bars: 10 and 1 μm in inset. The results indicate that exit of c-Kit from early endosomes **(B)** and its entry into late endosomes/MVBs **(A)** occurred at a similar rate in the two cell genotypes, whereas exit of c-Kit from late endosomes/MVBs **(A)** was delayed in *SMAP1*-targeted cells.
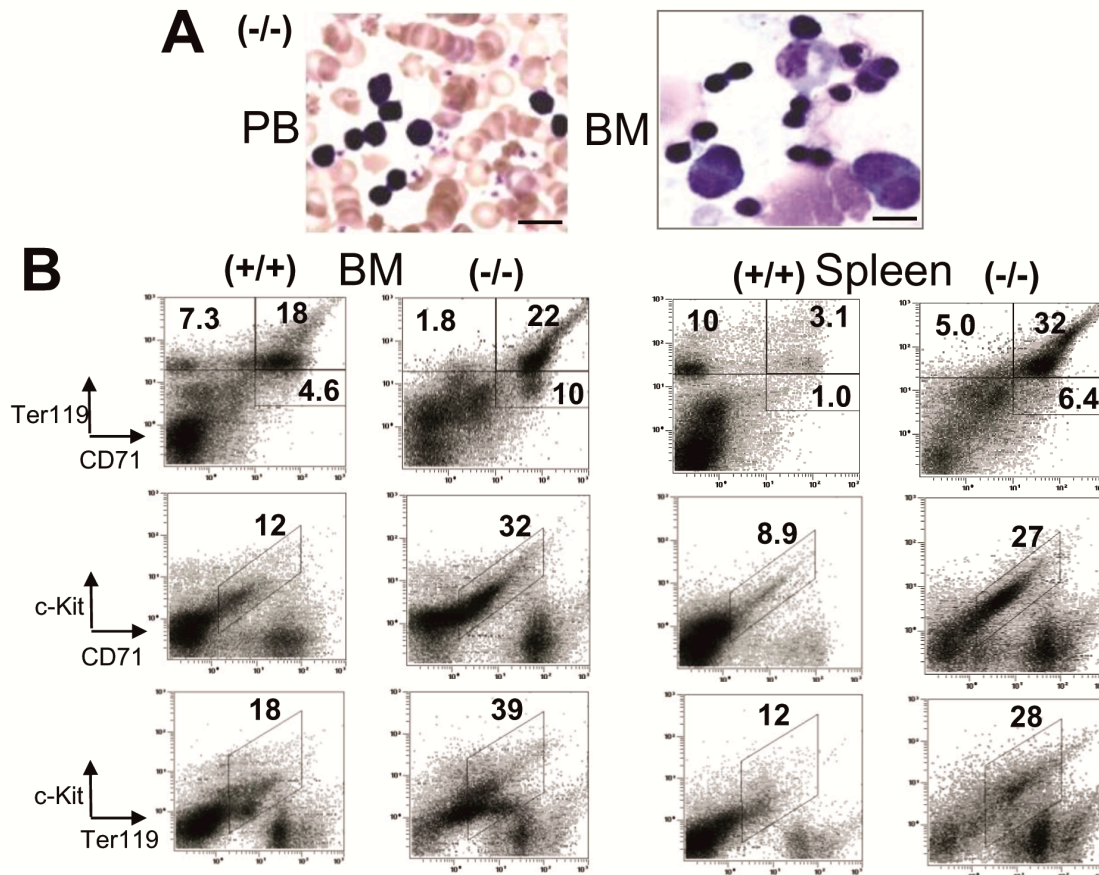
3

Supplemental Figure 3. Involvement of ArfGTPase in the transport of c-Kit from MVBs to lysosomes. COS7 cells were cotransfected with EYFP-c-Kit and Arf1Q71A, Arf5Q71A, or Arf6Q67A (these are dominant active forms of Arf), incubated in the presence of SCF for 30 min and processed for triple fluorescence detection of c-Kit, Hrs and Arf **(A)** or c-Kit, lysotracker and Arf **(B)**. The colocalization of the two molecules (c-Kit and Hrs in **A,** and c-Kit and lysotracker in **B**) was analyzed and plotted as histograms. Data are shown as averages ± sd (n=50–70). Arrows indicate the colocalization of three molecules (white in **A**) and two molecules (yellow in **B**). Scale bar: 10 μm. In mock-transfected cells, c-Kit was not colocalized with Hrs, whereas a large fraction of c-Kit colocalized with lysotracker, indicating the transport of c-Kit from MVB to lysosomes. In contrast, in Arf-overexpressing cells, a large fraction of c-Kit colocalized with Hrs but not with lysotracker, indicating the delay or block of c-Kit exit from MVB. This is likely an analogous situation to that seen in *SMAP1*-deficient cells, and suggests the involvement of Arf in the transport pathway of c-Kit from the MVB.

Supplemental Figure 4. Survival curves and appearance of ill-health conditions in *SMAP1*-targeted mice. **(A)** Kaplan–Meier curves were plotted for up to 35 months. Survival percentages were calculated for *SMAP1*(+/+), (+/-) and (-/-) mice (n = 14, 28, and 46, respectively). **(B)** Percentages of mice showing ill-health conditions. "Ill-health" was defined based on signs of general weakness, reduced motion, and shrunk posture, and judged by the observer blinded to genotypes.

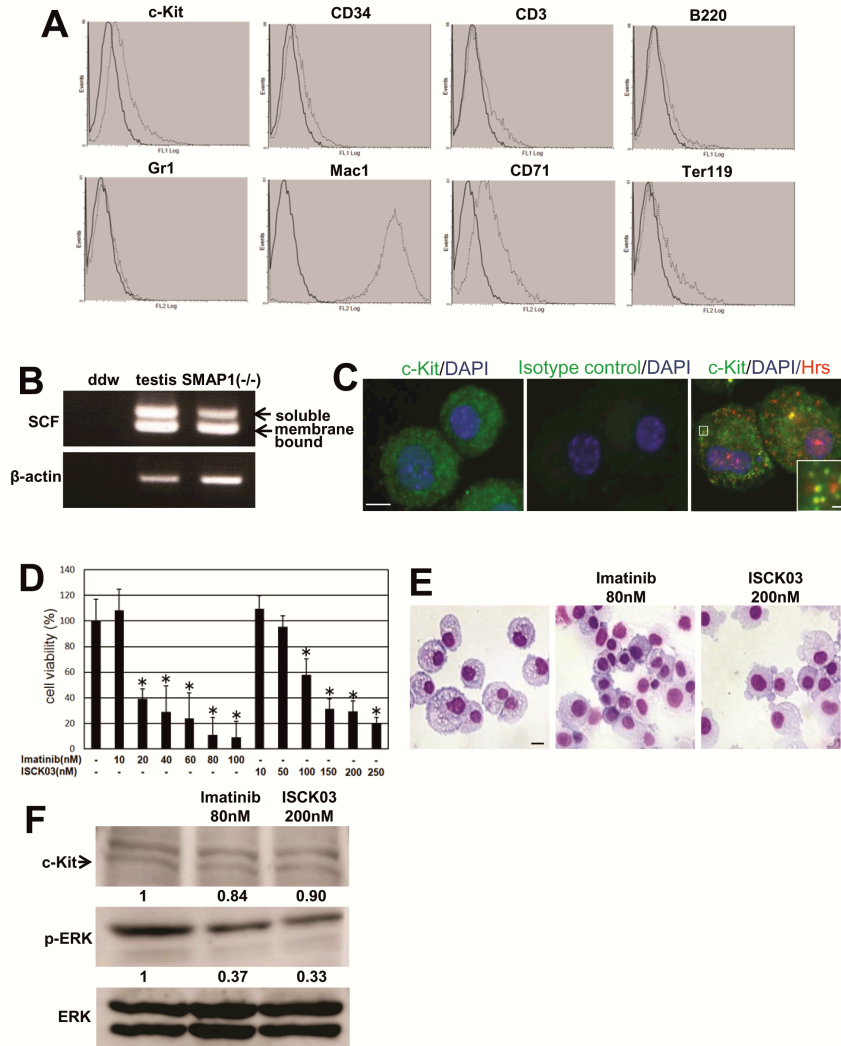**Supplemental Figure 5.** CFU-C assay of bone marrow cells. Cells from mice younger than 1 year, wild-type mice, and *SMAP1*(-/-) mice were assayed in vitro for their CFU-C activity. Four independent pairs of *SMAP1*(+/+) and (-/-) mice were used. No significant differences in BFU-E activity were detected between the two genotypes (see Figure 7H as comparison).

Supplemental Figure 6. Erythroleukemia in a *SMAP1*(-/-) mouse (ID number 192). **(A)** Smears of peripheral blood and bone marrow cells. Cells with densely stained nuclei represent erythroblasts. Among them, the large cells are megaloblasts. Scale bar: 10 μm. **(B)** Flow cytometry analyses of bone marrow cells and splenocytes. CD71^{hi}Ter119^{med} are proerythroblasts, CD71^{hi}Ter119^{hi} are basophilic erythroblasts, and CD71^{+}c-Kit^{+} and Ter119^{+}c-Kit^{+} are erythroid progenitors. In each fraction, higher percentages were calculated in *SMAP1*(-/-) compared to wild-type samples, indicating a substantial expansion of erythroid lineage cells.
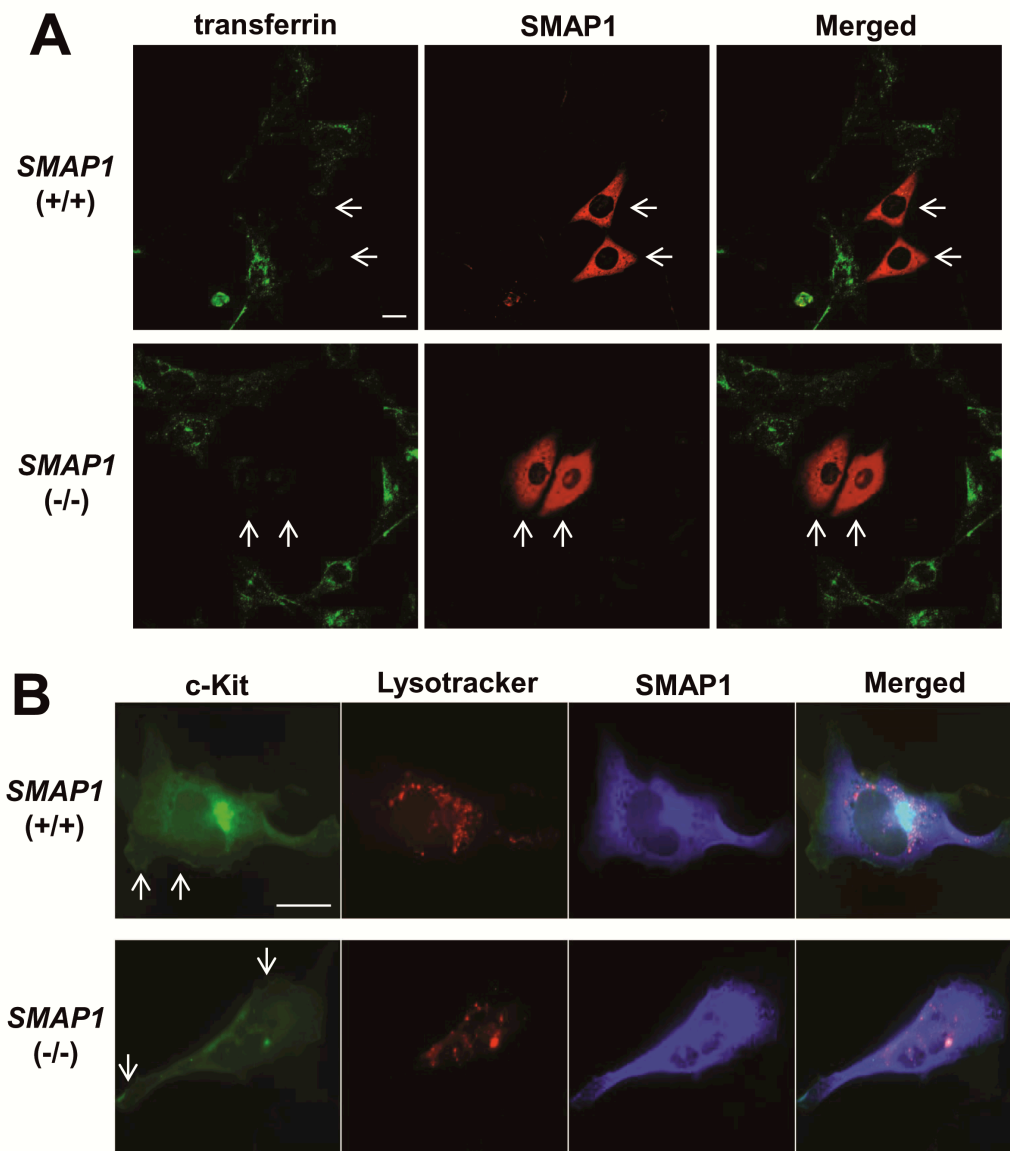
Supplemental Figure 7. MPD in a *SMAP1*(-/-) mouse (ID number 448). **(A)** Smears of peripheral blood and bone marrow cells. Note the presence of neutrophils in addition to the dysplastic red blood cells in the peripheral blood. The bone marrow appeared to contain large numbers of neutrophils and myeloblasts. Scale bar: 10 μm. **(B)** Flow cytometry analyses of bone marrow cells. Note the Gr1^{hi}Mac1^{+} (granulocytes), Gr1^{med}Mac1^{+} (monocytes), and Mac1^{+}c-Kit^{+} (myeloblasts) subfractions. In each subfraction, higher percentages of *SMAP1*(-/-) cells compared to wild-type cells were detected, indicating a substantial expansion of myeloid lineage cells.

Supplemental Figure 8. Involvement of c-Kit signaling in the growth of *SMAP1*(-/-) cells. The cell line used here was derived from the bone marrow of a monocytic AML mouse (ID 831). **(A)** Flow cytometry analysis of cell surface expression of various markers. Note that the cells were positive for c-Kit^{lo}, Mac1^{hi}, and CD71^{lo}, and negative for CD3, B220, Gr1 and Ter119. Thick lines indicate staining with isotype control IgG. **(B)** RT-PCR analyses of *SCF* transcripts. In the *SMAP1*(-/-) cell line, both soluble and membrane-bound isoforms of *SCF* transcripts were detected. Testis served as a positive control. **(C)** Double immunofluorescent staining of c-Kit and Hrs. Colocalization of c-Kit and Hrs at the MVB was evident. Scale bars: 10 and 1 μm in inset. **(D, E, F)** Effects of imatinib (a tyrosine kinase inhibitor) and ISCK03 (a c-Kit inhibitor) on the growth of *SMAP1*(-/-) cells. In **(D)**, cell viability was measured after a 24 h incubation using the CCK-8 assay kit. In **(E)**, apoptotic cells with dense nuclei and cytoplasmic blebs were evident in imatinib- and ISCK03-treated cells. In **(F)**, 80 nM imatinib and 200 nM ISCK03 had no significant effect on the level of c-Kit but significantly reduced the level of ERK1/2 phosphorylation to 37% and 33%, respectively. Collectively, these results suggest the positive involvement of c-Kit signaling in the growth of the *SMAP1*(-/-) AML-derived cell line.

9

Supplemental Figure 9. Effects of SMAP1 overexpression on transferrin incorporation and c-Kit endocytosis. **(A)** The *SMAP1*(+/+) and (-/-) MEFs were transfected by SMAP1, incubated with fluorescent-transferrin for 15 min. The arrows indicate the inhibition of transferrin uptake in cells transfected with SMAP1. **(B)** The *SMAP1*(+/+) and (-/-) MEFs were cotransfected with EYFP-c-Kit and SMAP1, stimulated with SCF for 30 min. Exogenous expression of SMAP1 blocked the internalization of c-Kit and caused its retention in the plasma membrane as highlighted by arrows. Therefore, simple put-back experiments of *SMAP1* into *SMAP1*(-/-) MEF did not work well for the purpose of rescuing defects of c-Kit transport observed in Figure 5. Scale bar: 10 μm.

Supplemental Table 1. Peripheral blood counts of individual *SMAP1*(-/-) mice diagnosed as MDS/AML

	Mouse ID	RBC (10^4/µl)	Hematocrit (%)	Hemoglobin (g/dL)	MCV (fl)	MCH (pg)	Reticulocytes (%)	PLT (10^4/µl)	WBC (10^2/µl)
MDS	47	734	34.5	11.4	53.1	13.8	13.9	89.8	83.0
	675	655	32.9	10.2	50.2	15.6	12.5	82.7	41.7
	834	714	33.2	10.1	46.5	14.1	12.5	68.1	164.0
	826	853	41.7	13.2	47.8	15.1	33.4	95.7	99.0
	524	822	40.7	13.0	49.5	15.8	N.D	122.0	56.0
	231	643	34.0	10.7	52.9	16.6	N.D	82.1	130.0
	576	647	38.5	10.7	59.5	16.5	25.1	183.4	84.7
	69	845	42.3	13.5	49.4	15.4	13.4	5.2	77.9
	72	452	24.0	6.3	53.1	14.1	N.D	86.2	138.0
	199	677	34.9	11.2	51.6	16.5	N.D	N.D	132.0
MPD/ MDS	448	826	45.2	15.1	54.7	18.3	N.D	14.9	209.0
	518	729	39.1	12.8	53.6	17.6	N.D	75.8	193.0
AML[a]	987	771	39.6	13.0	51.4	15.9	5.5	124.0	176.0
	831	833	38.0	12.1	45.6	14.4	12.5	308.2	150.2
	138	651	32.0	10.8	49.2	16.6	12.5	17.8	167.0

[a]We did not measure peripheral blood counts for the no. 34 and 192 *SMAP1*(-/-) mice that were diagnosed as having AML (see Table 1 as well).